Paracrine Regulation of Glucagon Secretion: The β-α-δ Model

M. Watts, J. Ha, O. Kimchi, and A. Sherman

Abstract

The regulation of glucagon secretion in the pancreatic α-cell is not well understood. It has been proposed that glucose suppresses glucagon secretion either directly through an intrinsic mechanism, within the α-cell, or indirectly through an extrinsic mechanism. We previously described a mathematical model for isolated pancreatic α-cells and used it to investigate possible intrinsic mechanisms of regulating glucagon secretion. We demonstrated that glucose can suppress glucagon secretion through both ATP-dependent potassium channels (K(ATP)) and a store-operated current (SOC). We now develop an islet model that combines previously published mathematical models of α- and β-cells with a new model of δ-cells and use it to explore the effects of insulin and somatostatin on glucagon secretion. We show that the model can reproduce experimental observations that the inhibitory effect of glucose remains even when paracrine modulators are no longer acting on the α-cell. We demonstrate how paracrine interactions can either synchronize α- and δ-cells to produce pulsatile oscillations in glucagon and somatostatin secretion or fail to do so. The model can also account for the paradoxical observation that glucagon can be out of phase with insulin while α-cell calcium is in phase with insulin. We conclude that both paracrine interactions and the α-cell's intrinsic mechanisms are needed to explain the response of glucagon secretion to glucose.

Keywords: insulin, pancreatic α-cell, glucagon, islet, somatostatin, pancreatic δ-cell

Introduction

Pancreatic islets consist of three main endocrine cell types that work together to control glucose homeostasis: α-cells, β-cells, and δ-cells. Pancreatic α-cells release glucagon primarily in response to low blood glucose levels, while pancreatic β-cells secrete insulin when blood glucose is elevated. Pancreatic δ-cells release somatostatin, which is an inhibitor of both insulin and glucagon secretion. Although glucose stimulated insulin secretion is relatively well understood, glucose suppression of glucagon secretion remains a puzzle (1).

Does glucose suppress glucagon secretion directly through intrinsic mechanisms or indirectly through extrinsic mechanisms? This question is part of an ongoing debate in α-cell dynamics. There is evidence that glucose can directly regulate glucagon secretion through ATP-sensitive K^+ (K(ATP)) (2) channels or a store-operated current (SOC) (3). However, there is also evidence that islet cells release a variety of factors that can modulate glucagon secretion, such as insulin (4, 5), Zn^+ (6, 7), γ-amino butyric acid (GABA) (8–10), and somatostatin (11–13).

We previously investigated intrinsic mechanisms of regulating glucagon secretion and showed that both K(ATP) channels and SOC are capable of suppressing glucagon secretion, albeit in different ways (14). Following the hypothesis of (2), K(ATP) channels suppress secretion in the model by closing when glucose raises the ATP/ADP ratio, as in β-cells. In contrast to β-cells, however, the resulting depolarization reduces spike amplitude by inactivating Na^+ and Ca^{2+} channels. This decreases Ca^{2+} influx and reduces glucagon secretion. Following the hypothesis of (3), glucose regulates glucagon secretion in the model through SOC by activating the sarcoendoplasmic reticulum calcium ATPase (SERCA), which pumps Ca^{2+} in to the endoplasmic reticulum (ER). When glucose is elevated, the ER fills, turning off SOC, and the consequent hyperpolarization reduces secretion. While the electrical effects of the two mechanisms are opposite, we proposed that SOC and K(ATP) work together to modulate glucagon secretion. For that model of α-cell dy-

namics, we neglected the role of paracrine inhibitors of glucagon secretion in order to focus on the intrinsic mechanisms.

In this study, we investigate how insulin and somatostatin can regulate glucagon secretion by combining previously published mathematical models of α- (14) and β-cells (15, 16) with a new model of δ-cells to create an islet model: the β-α-δ (BAD) model. We show that the model can reproduce experimental data demonstrating that the inhibitory effect of glucose remains even when paracrine modulators do not act on the α-cell. Based on this finding, we conclude that the role of paracrine interactions in the islet is to modulate the α-cell's intrinsic response to glucose. We also demonstrate how paracrine interactions synchronize α-cells in order to produce pulsatile oscillations in glucagon secretion. We find that the pancreatic β-cells serve as a pacemaker for the islet to drive oscillations in glucagon and somatostatin secretion.

Materials and Methods

Model

The β-α-δ (BAD) model for pancreatic islets contains one representative cell of each type (extended to several α-cells for Fig. 9) as well as the interactions between them (Fig. 1). β-cells are coupled by gap junctions, allowing individual β-cells to synchronize. Therefore, the model β-cell represents all of the β-cells in the islet. However, α- and δ-cells are not coupled by gap junctions, so the α- and δ-cells in the model represent the average behavior of the cells of their respective types, which may all be doing different things.

Pancreatic β-cells secrete by exocytosis of insulin containing granules, which involves a cascade of complex steps such as docking, priming, fusing, and release of insulin. A detailed kinetic model for insulin secretion that includes these processes was developed by Chen et al. (17). We now add this model of exocytosis to the dual oscillator model for pancreatic β-cells described previously in (15, 16). The dual oscillator model contains three interacting components, electrical/Ca^{2+}, glycolytic, and mitochondrial, that

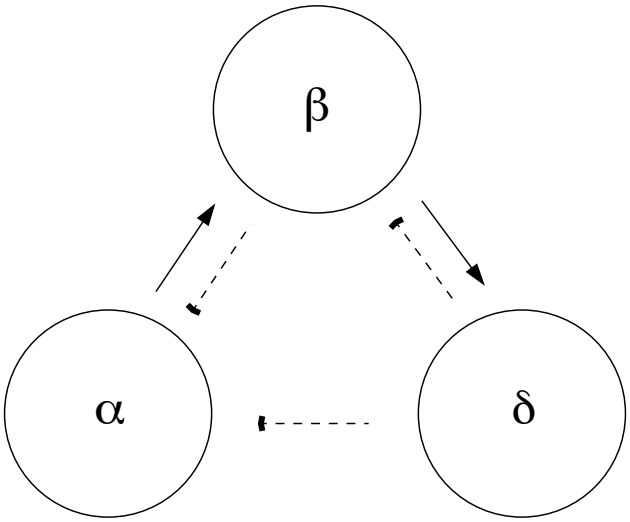

Figure 1: Paracrine interactions among α-, β- and δ-cells in the pancreatic islet. Solid lines with arrowheads indicate stimulation; dashed lines with blunt ends indicate inhibition.

combine to produce slow oscillations in membrane potential, cytosolic Ca^{2+} and metabolism. With the addition of the exocytosis model, insulin secretion also oscillates. For some simulations (Figs. 3, 4) that do not involve oscillations, a simplified electrical spiking model was used.

The α-cell model is taken from (14). The contribution of K(ATP) channels to glucagon secretion is the same as in (14). Fig. 2A shows the behavior of the α-cell as a function of the K(ATP) conductance, $g_{K(ATP)a}$; the subscript *a* denotes that this is the conductance in the α-cell. The lines represent constant voltages, and the circles represent the minimum and maximum voltages during spiking. As glucose is increased, $g_{K(ATP)a}$ decreases, and action potentials are produced. Figure 2B reprises from (14) the fundamental feature of α-cell secretion: as $g_{K(ATP)a}$ decreases, glucagon secretion first increases then decreases. The increase is due to the initiation of spiking, whereas the decrease results from reduced spike amplitude, and ultimately loss of spiking, as Na^+ and Ca^{2+} channels inactivate.

The contribution of SOC (not shown) is qualitatively the same as in (14), but the conductance has been made an order of magnitude smaller; we show below that this is sufficient to account for data on secretion in the absence of K(ATP) channels and when SERCA is blocked. At very low $g_{K(ATP)a}$ the cell settles on a

depolarized plateau that does not support secretion.

Finally, we have added a kinetic model of exocytosis, similar to the one used for the β-cells. Inhibition of granule priming due to reduction of cAMP by somatostatin will play a key role in the simulations here.

The δ-cell model is adapted from the α-cell model. We remove the T-type Ca^{2+} current, which is absent in mouse δ-cells (18), and modify the parameters of the remaining ionic currents to shift the dependence of the electrical activity to the left. The dependence of the electrical activity as a function of the δ-cell K(ATP) conductance, $g_{K(ATP)d}$, is shown in Fig. 2C. As in the α-cell, action potentials are produced when $g_{K(ATP)d}$ is decreased, but there is limited inactivation even when K(ATP) conductance is 0. As a result, somatostatin secretion monotonically increases as $g_{K(ATP)d}$ decreases (Figure 2D). Accordingly, somatostatin secretion monotonically increases with glucose. Somatostatin secretion is modeled as a function of microdomain Ca^{2+} (Eq. 30 in the Appendix).

Equations and parameters not described here for the three cell types are located in the Appendix.

While each cell type has its own set of electrical, calcium, and secretion equations, we make the simplifying assumption that insulin, glucagon, and somatostatin are secreted into a common, well-mixed space. The concentrations of insulin (I), glucagon (G), and somatostatin (S) in this compartment are given by the following equations:

$$\frac{dI}{dt} = \frac{J_{IS}}{v_c} - f_b I \tag{1}$$

$$\frac{dG}{dt} = \frac{J_{GS}}{v_c} - f_a G \tag{2}$$

$$\frac{dS}{dt} = \frac{J_{SS}}{v_c} - f_d S \tag{3}$$

where J_{IS} is the rate of insulin secretion, J_{GS} is the rate of glucagon secretion, J_{SS} is the rate of somatostatin secretion, v_c is the volume of the compartment, and f_b, f_a, and f_d are the rates of hormone clearance from the compartment.

Next we describe the interactions between the cells that are included in the model. The β-cell modifies

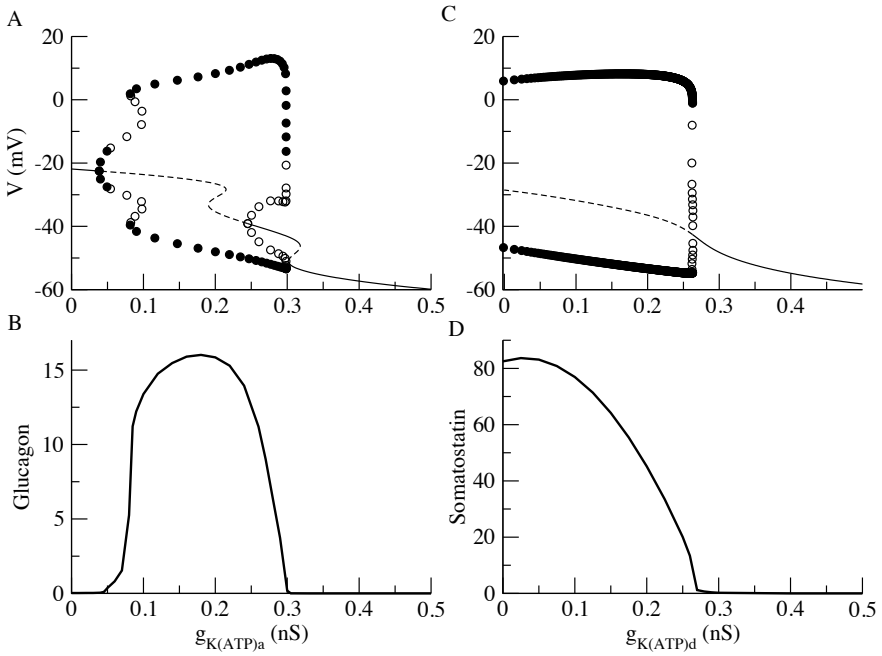

Figure 2: Bifurcation analysis of the α- and δ-cell models. (A) Bifurcation diagram of the α-cell model with $g_{K(ATP)a}$ as the bifurcation parameter. The solid curve represents stable steady-state solutions, while the solid circles are stable spiking solutions with the maximum and minimum voltages plotted. The dashed curve represents unstable steady-state solutions and the open circles unstable periodic solutions. (B) As glucose increases, $g_{K(ATP)a}$ decreases and glucagon secretion first increases then decreases. (C) Bifurcation diagram for the δ-cell model. (D) As $g_{K(ATP)d}$ decreases, somatostatin secretion increases monotonically.

glucagon secretion by increasing K(ATP) channel activity (7, 19); therefore, the conductance of the α-cell K(ATP) channels ($g_{K(ATP)a}$) depends on the concentration of insulin in the common space. The equation for $g_{K(ATP)a}$ is

$$g_{K(ATP)a} = \bar{g}_{K(ATP)a}\, EffI_a \tag{4}$$

where $EffI_a$ is the effect of insulin on the α-cell and $\bar{g}_{K(ATP)a}$ is the maximal conductance of the K(ATP) channels. $EffI_a$ is an increasing function of insulin and is given by the following phenomenological equation

$$EffI_a = 0.0015/(1+\exp(-(I-1500)/200)) + k_a. \tag{5}$$

We neglect the recently described additional effect of insulin to lower cAMP (20), which is subsumed under the effects of somatostatin (see below). The implications of a separate effect of insulin on cAMP will be addressed in the Discussion.

There is also evidence that the β-cell stimulates somatostatin secretion (21). Moreover, one of the implications of our simulations is that synchrony between insulin and somatostatin is only possible if β-cells stimulate δ-cells. One possible mechanism is a Cl^- channel activated by GABA. It has been shown in both rat and human islets that GABA is co-released with insulin in large-dense core granules (22, 23). For simplicity, instead of adding equations for GABA, we model the conductance of the GABA current as depending on insulin. I_{GABA} is given by the following equation

$$I_{GABA} = \bar{g}_{GABA}\, \mathit{EffI}_d (v_d - v_{GABA}) \tag{6}$$

where EffI_d is the effect of GABA on the δ-cell, $\bar{g}_{GABA}$ is the maximal conductance of the GABA channel, and v_{GABA} is the reversal potential. Because GABA is co-released with insulin, we assume that GABA is an increasing function of insulin and model EffI_d by the following equation

$$\mathit{EffI}_d = 0.8/(1+\exp(-(I-1500)/500)). \tag{7}$$

Somatostatin inhibits insulin and glucagon secretion through both G protein-coupled inwardly-rectifying potassium (GIRK) channels and a direct effect on exocytosis (24–27). The GIRK current I_{GIRKx} is given by the following equation

$$I_{GIRKx} = \bar{g}_{GIRKx}\, \mathit{EffS}_x (v_x - v_{GIRK}) \tag{8}$$

where $x = a, b$ for the α- or β-cell respectively, EffS_x is the effect of somatostatin, $\bar{g}_{GIRKx}$ is the maximal conductance of GIRK, and v_{GIRK} is the reversal potential. EffS_x is an increasing function of somatostatin and is given by the following equation

$$EffS_x = 1/(1+\exp(-(S-35)/10)). \tag{9}$$

Somatostatin inhibits exocytosis both by inhibiting adenylate cyclase, which lowers cAMP levels (28, 29), and through a pathway independent of cAMP (25, 27). In the model, somatostatin inhibits exocytosis by increasing the parameter that governs the rate of depriming of granules, r_{-2x}, where $x = a,b$ for α or β-cell. The equation for r_{-2x} is

$$r_{-2x} = r_x/(1+\exp(-S+35)). \tag{10}$$

Similar results would be obtained if somatostatin were assumed to reduced the rate of priming r_{2x}. See Eq. 18 in the Appendix for additional equations governing exocytosis.

Glucagon increases insulin secretion by increasing cAMP levels (29–31). In the model, glucagon increases the parameter that governs the rate of priming granules, $r_{2,b}$. The equation for $r_{2,b}$ is

$$r_{2,b} = \left(\frac{0.004}{1+\exp(-G+15)} + 0.006\right)\left(\frac{c_b}{c_b+K_p}\right). \tag{11}$$

Similar results would be obtained if glucagon were assumed to increase the rate of resupplying granules, $r_{3,b}$ (see Eq. 19 in the Appendix).

The differential equations were solved numerically with the variable step size method CVODE implemented in the XPPAUT software package (32) with absolute and relative tolerances 10^{-10}.

Results

Effect of Somatostatin on Glucagon Secretion

The role of somatostatin as an inhibitor of glucagon secretion was recently studied in Cheng-Xue et al. (33) using somatostatin knockout islets ($Sst^{-/-}$). It was shown that the absence of somatostatin resulted

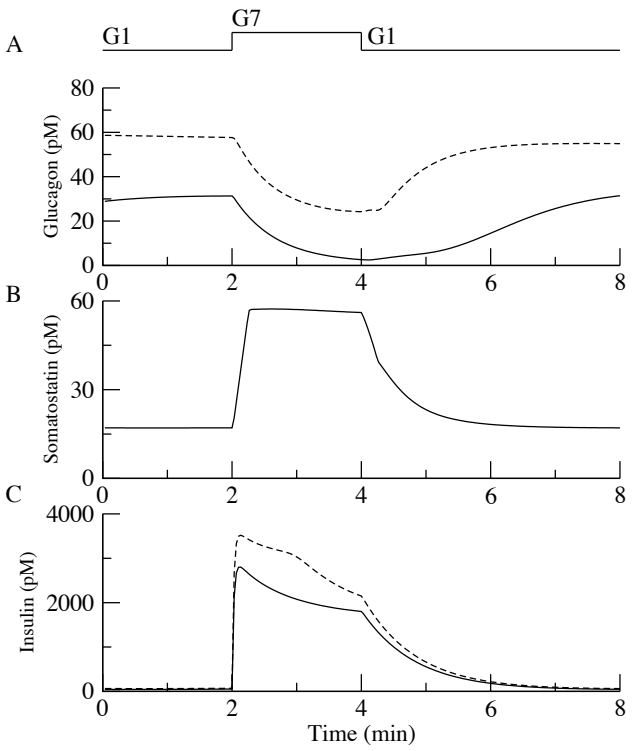

Figure 3: Somatostatin tonically inhibits both glucagon and insulin secretion. In $Sst^{+/+}$ islets (solid curve), increasing glucose decreases glucagon secretion (A), while increasing somatostatin (B) and insulin secretion (C). While insulin and glucagon are both higher in $Sst^{-/-}$ islets (dashed curve) (A,C), glucose still retains its inhibitory effect on glucagon secretion. Compare to Fig. 4 in (33). Parameters for G1: $\bar{g}_{K(ATP)a}$ = 30 nS, $g_{K(ATP)b}$ = 150 pS, $g_{K(ATP)d}$ = 0.26 nS, $k_{SERCA} = 0.05$. G7: $\bar{g}_{K(ATP)a} = 27$ nS, $g_{K(ATP)b} = 70$ pS, $g_{K(ATP)d} = 0.22$ nS, $k_{SERCA} = 0.5$. $\bar{g}_{SOC} = 0.025$ nS throughout.

in an overall increase in glucagon secretion, but the inhibitory effect of glucose remained. Our model can reproduce the main features of this experiment, as shown in Fig. 3. In $Sst^{+/+}$ islets increasing glucose from 1 mM (G1) to 7 mM (G7) decreases glucagon secretion (Fig. 3A, solid curve), while increasing somatostatin and insulin secretion (Fig. 3B,C). While glucagon secretion is higher in $Sst^{-/-}$ islets, glucose is still able to inhibit secretion (Fig. 3A, dashed curve). $Sst^{-/-}$ islets are modeled by fixing $\bar{g}_{GIRKx}$ to 0 and r_{-2x} to 0.001, removing the effects of somatostatin from the islet. Increasing the glucose concentration decreases the conductance of the K(ATP) channels for all three islet cell types. For this simulation, we assume for simplicity that there are no metabolic oscillations and K(ATP) conductance is constant. Therefore, the change in glucose concentration was modeled as a change in $\bar{g}_{K(ATP)a}$, $g_{K(ATP)b}$, and $g_{K(ATP)d}$, where

$$I_{K(ATP)x} = g_{K(ATP)x}(V - V_K),$$

$x = a, b, d$, and $g_{K(ATP)a}$ is given by Eq. 4.

Pancreatic α-cells have also been proposed to contain a store-operated current (SOC), which is affected by increasing glucose. SOC is an inward current with a conductance that decreases as ER Ca^{2+} increases:

$$g_{SOC} = \bar{g}_{SOC} c_{er\infty}(C_{er}), \tag{12}$$

where $c_{er\infty}$ represents C_{er}-dependent activation. In low glucose the ER is relatively depleted because of limited SERCA activation. Increasing glucose activates SERCA and fills the ER, which reduces SOC. This effect of SERCA activity was modeled by a change in the rate of SERCA pump activity, k_{SERCA} (See Eq. 23 in the Appendix). Although somatostatin no longer affects the islets in this simulation, glucose still inhibits glucagon secretion through the closure of K(ATP) channels, the inactivation of a store-operated current (SOC), and insulin.

Although SOC is present in Fig. 3, it does not play a major role in reducing glucagon secretion, but another experiment in (33) showed that glucose still suppressed glucagon secretionin the absence of K(ATP) channels and somatostatin, using $SUR1^{-/-}$ islets and pertussis toxin (PTX). Based on this data, it was argued that there exists another mechanism that contributes to glucose suppression of glucagon secretion. We proposed previously (14) that this unknown mechanism is SOC, we now extend this by including paracrine effects. In addition, we found that SOC can be effective even with much smaller conductance (0.015 nS) than was used in (14).

The first step in modeling $SUR1^{-/-}$ islets is to remove the K(ATP) current. However, in the absence of any other change, this would result in α-cells that are permanently depolarized. We propose that some other K^+ conductance must be up-regulated to prevent this from happening. We therefore replaced K(ATP) with a constant K^+ conductance (0.28 nS). Figure 4A shows that glucose can suppress secretion in the absence of K(ATP) channels both with (solid line) and without (dashed line) the inhibitory effect of somatostatin

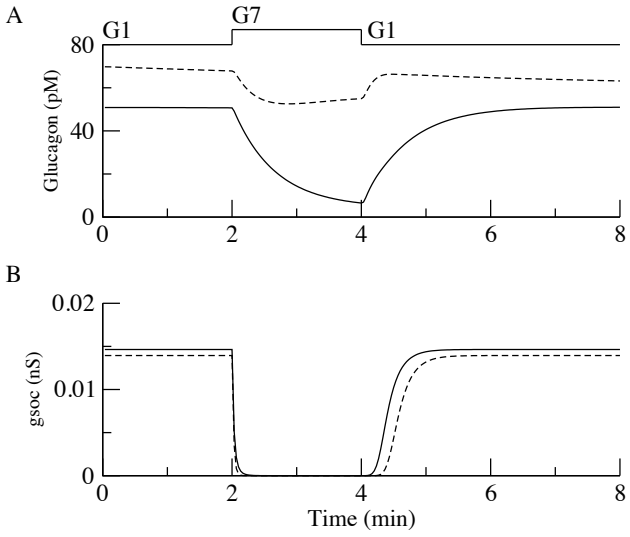

Figure 4: Glucose can inhibit glucagon secretion through SOC, independently of K(ATP) channels, somatostatin, and insulin. (A) Glucose can inhibit secretion in islets without functional K(ATP) channels (solid curve), and in islets without functional K(ATP) channels or somatostatin (dashed curve). (B) $\bar{g}_{SOC} = 0.025$ nS, as in Fig. 3. In G1 k_{SERCA} = 0.05 ms^{-1}, making $g_{SOC} \approx 0.015$ nS. In G7 $k_{SERCA} = 0.5$ ms^{-1}, making g_{SOC} decrease to 0. $\bar{g}_{K(ATP)a}$ is replaced by a constant background K^+ conductance of 0.28 nS, and $g_{K(ATP),d}$ is replaced by a constant K^+ conductance of 0.26 nS. Somatostatin secretion is assumed to respond to glucose via a K(ATP)-independent amplifying factor (34) (see Eq. 31 in the Appendix).

by deactivating SOC current. Figure 4B shows that only a small SOC curreent is needed: it is sufficient to assume that g_{SOC} is around 0.015 nS in 1 mM glucose and decreases to zero in 7 mM glucose.

The simulations of Figs. 3, 4 suggest that, although somatostatin and insulin have large effects on α-cells, these paracrine factors are not themselves responsible for the glucose sensitivity of glucagon secretion. We address this further in the Discussion.

Synchronized Hormone Oscillations

We now investigate the role of paracrine effects in hormone oscillations, which have been recorded in high glucose (20 mM) in both isolated islets and the perfused rat pancreas (35–38). Insulin and somatostatin oscillate in-phase with each other, but out-of-phase with glucagon. To study this, we now include a glycolytic oscillator in the β-cells to drive insulin oscillations (see Eq. 16 in the Appendix). Figure 5 shows secretion

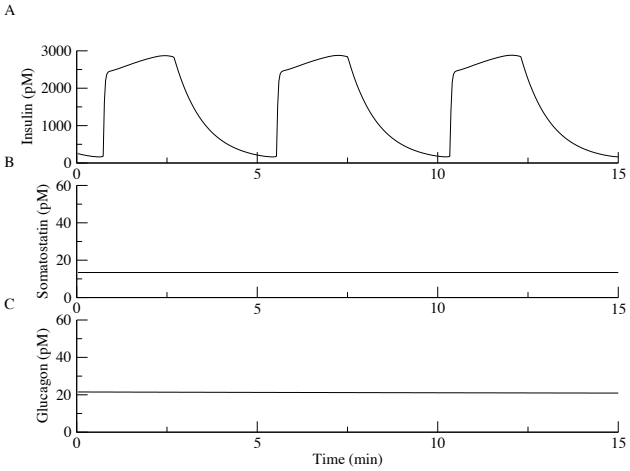

Figure 5: Secretion from isolated cells. (A) Oscillatory secretion in insulin from β-cells. (B&C) Static secretion in glucagon and somatostatin from α- and δ-cells.

using this augmented model,but without paracrine interactions, at an elevated level of glucose. In this case insulin secretion is oscillatory (Fig. 5A), but the secretion of somatostatin and glucagon is flat (Fig. 5B,C).

Pulsatile insulin secretion depends on two distinct characteristics of β-cells. First, insulin secretion is driven by an intrinsic oscillatory mechanism dependent on glucose metabolism and ion channels (39, 40). Second, within an islet, individual β-cells are coupled to neighboring β-cells by gap junctions (41–43). This coupling allows the β-cells to secrete in synchrony, and the intrinsic oscillation makes the secretion pulsatile. Glucagon and somatostatin secretion in the simulation of Fig. 5 are not pulsatile because the α-cell and δ-cell models lack an intrinsic slow oscillator, and can only produce spikes of action potentials. Although, Ca^{2+} oscillations have been observed in α-cells (44–47), these cells are not coupled by gap junctions like β-cells and are not synchronized. Below (Fig. 9), we will come back to the possibility that α-cells contain an intrinsic oscillatory mechanism, but first we examine whether paracrine interactions alone can account for oscillations in glucagon and somatostatin.

In the model, glucagon secretion is influenced both indirectly, through the postulated effects of insulin to open K(ATP) chanels, and directly, by the postulated effect of somatostatin to inhibit exocytosis (Fig. 1). Somatostatin is always inhibitory, independent of glucose concentration, but the direction of the insulin

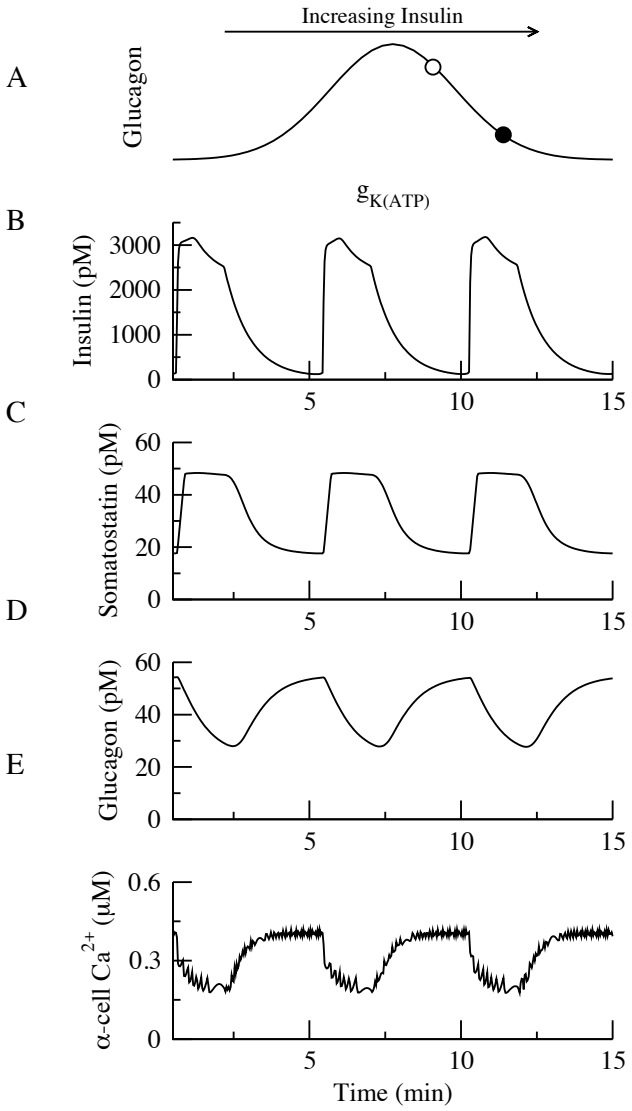

Figure 6: Oscillatory insulin secretion acts as a pacemaker to synchronize hormone oscillations. (A) The α-cell is assumed to sit on the right side of the bell (white circle), so insulin lowers α-cell Ca^{2+} when it increases $g_{K(ATP)}$ and decreases glucagon secretion (black circle). (B,C) In-phase insulin and somatostatin secretion. (D,E) Both Ca^{2+} and glucagon are anti-phase with insulin. In this simulation $k_a = 0.00889$ and $r_a = 0.1$. As insulin oscillates, $g_{K(ATP)a}$ varies between 0.24 and 0.28 nS.

effect is ambiguous. That is, the relationship between K(ATP) conductance and glucagon secretion was shown to be a bell-shaped function of the prevailing K(ATP) conductance (48). The intrinsic response of the isolated α-cell in the model similarly produces a bell-shaped curve as $g_{K(ATP)a}$ is varied, as shown in (14)

and repeated here in Fig. 2A. Thus, a glucose-mediated decrease in $g_{K(ATP)a}$ or an insulin-mediated increase in $g_{K(ATP)a}$ can either increase or decrease glucagon secretion, depending on the starting $g_{K(ATP)a}$ level.

In Fig. 6A, we assume that for the given level of glucose the α-cell sits on the right side of the bell-shaped curve (white circle). Then, increasing insulin lowers α-cell Ca^{2+} and decreases secretion (black circle, Fig. 6A). Consequently, both glucagon secretion and α-cell Ca^{2+} are anti-phase with insulin (Fig. 6D,E). Also, due to the stimulatory effect of the β-cell on somatostatin secretion, insulin and somatostatin oscillate in phase with each other (Fig. 6B,C).

A recent study, however, reported that α-cell Ca^{2+} is in-phase with β-cell Ca^{2+} at 20 mM glucose (49) and hence presumably in-phase with insulin. In Fig. 7A, we show that this can happen if the α-cell sits on the left-hand side of the bell (white circle, Fig. 7A). In this case, insulin increases α-cell Ca^{2+} by increasing $g_{K(ATP)}$. This would normally be expected to increase glucagon secretion (black circle), but somatostatin overcomes the effect of Ca^{2+} and is able to suppress glucagon secretion through its direct effect on exocytosis. Therefore, glucagon secretion is anti-phase with insulin (Fig. 7D), while Ca^{2+} is in-phase (Fig. 7E). As in Fig. 6, insulin and somatostatin secretion are in-phase with each other (Fig. 7B,C).

Although it may seem paradoxical for α-cell Ca^{2+} to be out-of-phase with glucagon, the configuration of Fig. 7 avoids another paradox that would afflict Fig. 6. In that case, $g_{K(ATP)}$ places the α-cell just to the right of the peak of the glucagon secretion curve in high glucose. That means that at low glucose, the physiologically relevant case, the α-cell would sit far to the right of the peak. Then, increases in glucose would increase glucagon secretion, unless counter-balanced by another effect. In low glucose, the paracrine inhibition from somatostatin would be relatively weak and limited in its ability to serve this function.

Oscillations in glucagon are not universally observed. For example, in (50) no oscillations were observed, and no synchrony among α- or δ-cells. Thus, while the structure of islet-cell interactions depicted in Fig. 1 is favorable for coordinated hormone oscillations, it is not sufficient. Fig. 8A-C shows one way that oscillations can fail to occur. If turnover of hormones in the interstitial space is too rapid, the concentration will not build up and dissipate slowly as insulin rises and falls. Another way oscillations could fail to appear is if the β-cells exhibit fast, rather than slow, electrical oscillations (Fig. 8D-F). In this case, insulin secretion

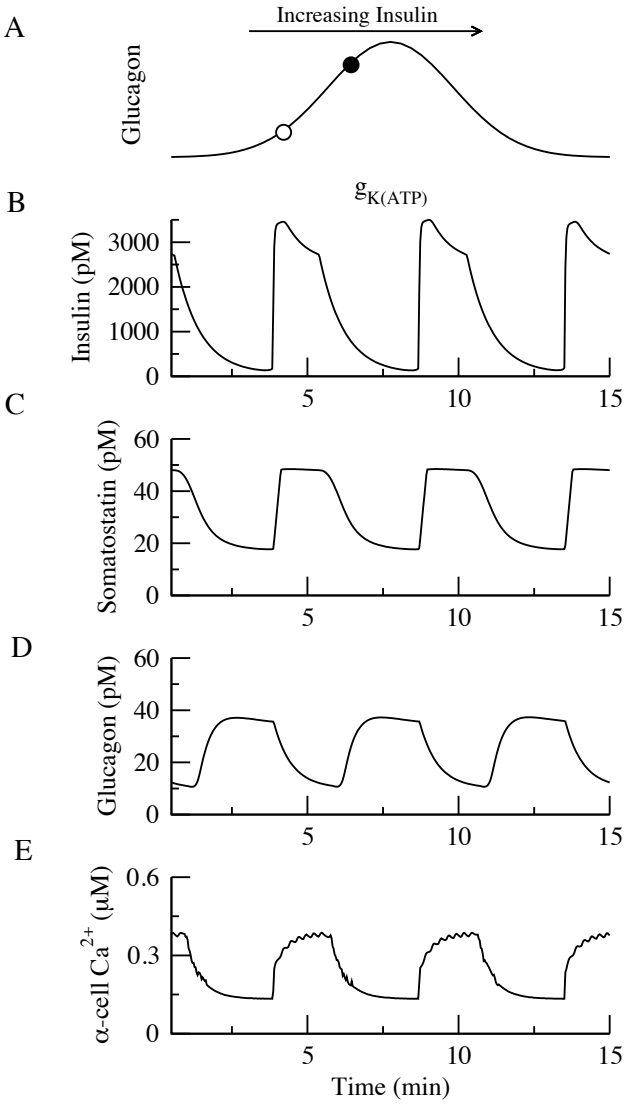

Figure 7: (A) The α-cell is assumed to sit on the left side of the bell-shaped dose-response curve in elevated glucose. Insulin increases α-cell Ca^{2+} by increasing $g_{K(ATP)}$. (B,C) In-phase insulin and somatostatin secretion. (D,E) Somatostatin suppresses glucagon secretion by a direct effect on exocytosis, which trumps the rise in Ca^{2+} so glucagon is anti-phase with insulin. In this simulation k_a = 0.00148 and r_a = 5. As insulin oscillates, $g_{K(ATP)a}$ varies between 0.04 and 0.08 nS. (Compare with Fig. 2A.)

does not exhibit slow oscillations, so glucagon and somatostatin cannot oscillate.

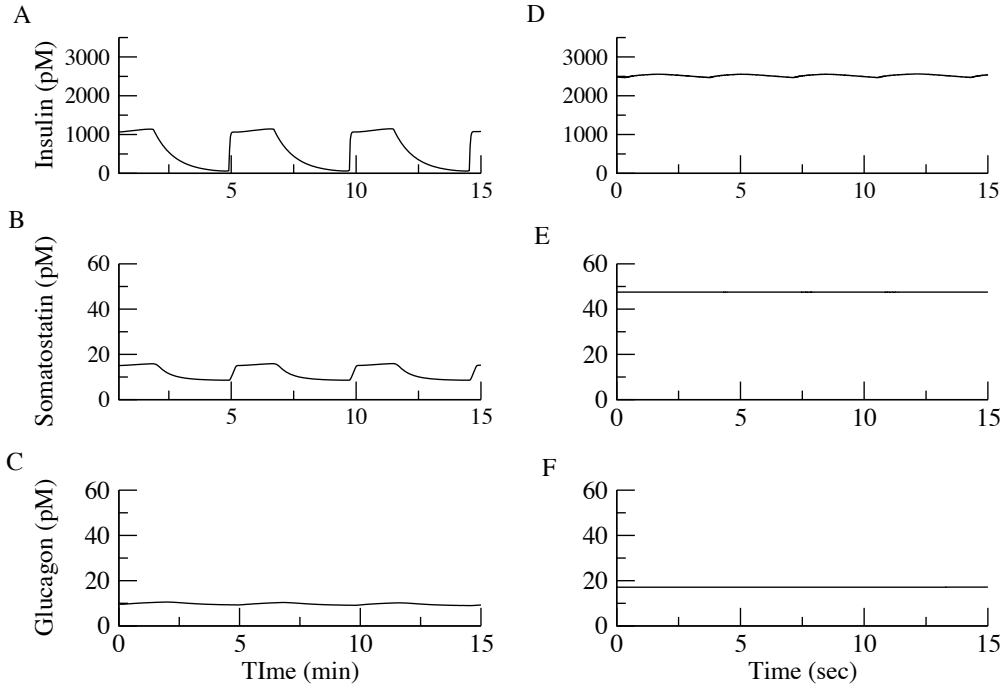

Figure 8: (A-C) Glucagon oscillations may not be observed if the turnover of harmones is too rapid. For this simulation the parameters for the flux out of the compartment were increased for all three harmones. (f_b=5000,f_a=300,f_d=0.006) (D-F) Glucagon does not oscillate if β-cells exhibit fast bursting oscillations. Note the time scale is now in seconds. ($g_{K(Ca)}$ = 500 pS, J_{GK}=0.8, $g_{K(ATP)b}$ = 8500 nS).

Intrinsic Glucagon Pulsatility

As stated earlier, there is some evidence that α-cells may contain an intrinsic glycolytic oscillator (44, 45, 51). However α-cells are extremely heterogeneous (46, 47, 52) and not coupled by gap junctions like β-cells. We propose that paracrine interactions are needed to synchronize glucagon oscillations even if some or all of the α-cells are intrinsically oscillatory. To test this hypothesis, we extend the model to include five α-cells in addition to the one representative β-cell and one representative δ-cell. The equations for the glycolytic oscillator from (15) were added to the α-cell model (see Eq. 16 in the Appendix). Heterogeneity was incorporated by giving each cell a different value for the parameter J_{GK}, which is the rate of the enzyme glucokinase, and κ, which controls the speed of the glycolytic oscillations; many other parameters could have been used for this illustration.

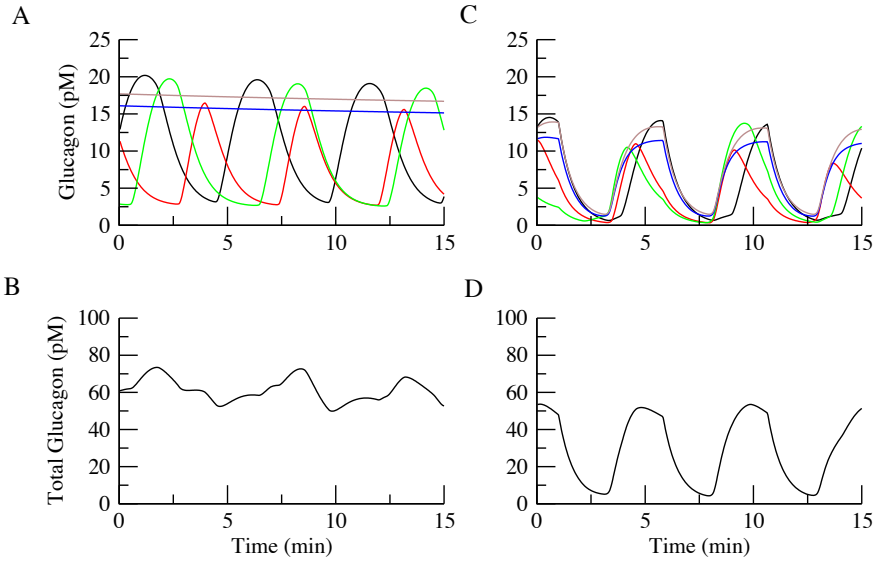

Figure 9: (A, B) If glucagon is secreted from 5 uncoupled α-cells, total glucagon secretion is flat. Paracrine effects suppressed by fixing $\bar{g}_{GIRK,a}$ to 0, $r_{-2,a}$ to 0.001, and $g_{K(ATP)a}$ to 27 nS. (C, D) However, if the same cells are coupled by paracrine effects, total glucagon secretion is oscillatory. α-cell heterogeneity was modeled by having different J_{GK} and κ values for the 5 α-cells: $J_{GK,a1}$=0.2, $J_{GK,a2}$=0.1, $J_{GK,a3}$=0.15, $J_{GK,a4}$=0.25,$J_{GK,a5}$=0.3, κ_{a1}=0.003, κ_{a2}=0.005, κ_{a3}=0.003, κ_{a4}=0.005, κ_{a5}=0.003.

Figure 9A shows the glucagon secretion from the five individual α-cells without the inhibitory effects of insulin or somatostatin. The lack of paracrine interactions was modeled by fixing the conductance of the GIRK and K(ATP) channels and the rate of depriming of granules in the α cells. Three of the α-cells are oscillating, while two are spiking but not undergoing slow oscillations. We include both oscillating and non-oscillating α-cells since it is likely that only a subset of individual α-cells contain oscillations in secretion. The total glucagon secretion from the islet is nearly static (Fig. 9B), and would be flatter still if more cells were included. However, if we run the same simulation and include the paracrine effects, glucagon secretion becomes pulsatile. In contrast to Fig. 9A, Fig. 9C shows that each individual cell is secreting in an oscillatory fashion and this secretion is synchronized. Since the individual α-cells are now synchronized, the total glucagon secretion is pulsatile (Fig. 9D). This indicates that another role of paracrine effects is to tame the heterogeneity of α-cells.

Discussion

This study continues the investigation begun in (14) on the roles of intrinsic and paracrine factors in the regulation of glucagon secretion. In the first paper, we showed that two intrinsic mechanisms, K(ATP) channels and SOC channels, could each account for the reduction of glucagon secretion by glucose. In the current study, we have added models for β- and δ-cells in order to investigate paracrine effects in intact pancreatic islets.

We have shown that this β-α-δ (BAD) model can account for experiments in which the effects of somatostatin are absent due to genetic knockout (Fig. 3) or pre-treatment with pertussis toxin (Fig. 4). In the latter case, K(ATP) channels were also absent (due to genetic knockout), but responsiveness to glucose remained. To the extent that insulin acts by modulating K(ATP) channels, this simulation also demonstrates that glucose can inhibit glucagon secretion independently of insulin secretion. The model shows that the residual glucose sensitivity could be accounted for by the effect of glucose to fill the ER and reduce SOC current.However, recent evidence suggests that insulin may act independently of K(ATP) channels, by reducing cAMP (20), so SOC may not be solely responsible for the decrease in secretion in the experiments corresponding to Fig. 4.

The model shows that SOC can effect glucagon secretion even when the conductance is rather small, much smaller than we previously used in (14).Thus, although there is no direct electrophysical evidence for the existence of SOC current in α-cells, it is possible that it would be difficult to detect experimentally unless other factors, such as somatostatin and K(ATP) channels, are absent or non-functional.

Another channel issue highlighted by Fig. 4 is that some other K^+ channel likely compensates for the loss of K(ATP) channels. Two possible candidates are TASK-1 (53) and GIRK (54). Similarly, it is not clear what mechanisms mediate the increase by glucose of somatostatin secretion in δ cells when K(ATP) is knocked-out. It has been suggested that calcium-induced calcium release increases somatostatin secretion provided K(ATP) conductance is reduced sufficiently (34). In the absence of detailed information about the pathway, we have simply assumed that secretion is amplified when glucose rises.

Our primary focus has been to demonstrate how islets produce pulses of insulin and somatostatin secretion in antisynchrony with those of glucagon. The relevant experiments were carried out at high glucose (20 mM), where we assume SOC is negligible.

Within an islet, β-cells are electrically coupled to their neighbors through gap junctions (41–43). This coupling allows the β-cells to secrete in synchrony, generating pulses of insulin secretion (Fig. 5). On the other hand, α- and δ-cells are not coupled through gap junctions, but we have shown that β-cells can synchronize and drive pulses of glucagon and somatostatin secretion.

For somatostatin to oscillate synchronously with insulin, β-cells must stimulate somatostatin secretion. In the model, this stimulation comes from GABA, which is co-secreted with insulin (22, 23) and modeled simply as proportional to insulin secretion. Other possible mechanisms include ATP (55) and urocortin3 (56) or any other paracrine factor that oscillates in synchrony with insulin. In the absence of such a mechanism, somatostatin secretion is static (Fig. 5B), since we assume that individual δ-cells produce spikes of electrical activity but no slow oscillations (some may (44), but in the absence of synchrony will not produce islet-wide pulsatility). However, somatostatin secretion oscillates in synchrony with insulin when the δ-cell is stimulated by the β-cell (Figs. 6B,C& 7B,C). Thus, β-cells can drive pulses of somatostatin secretion in sufficiently high glucose.

Like somatostatin, glucagon secretion is expected to be static when uncoupled from paracrine effects (Fig. 5C). We have shown that oscillations in glucagon secretion can be driven by the β-cell, but the δ-cell is needed to guarantee that these oscillations are out of phase with insulin. Under the assumption that insulin secretion modulates K(ATP) channels, its effect on the α-cell can change depending on the K(ATP) conductance in the absence of modulation by insulin. If the K(ATP) conductance is near or to the right of the peak of the bell-shaped curve, as in Fig. 6A, then increasing insulin would reduce secretion. Therefore, inhibition from insulin is all that is necessary to produce antisynchrous oscillations in glucagon secretion (Fig. 6D). However, if the α-cell K(ATP) conductance is far to the left of the peak, as in Fig. 7A, then increasing insulin would increase secretion. In this case, the inhibitory effect of somatostatin can overcome the rise in Ca^{2+} produced by the effect of insulin in order to produce anti-synchronous oscillations

in glucagon (Fig. 7D). Again, insulin could also contribute by reducing cAMP (20). However, oscillations in α-cell Ca^{2+} would be out of phase with glucagon secretion (Fig. 7E). Although this seems paradoxical, recall that the observations were made in high glucose; the configuration of Fig. 7 is more likely than that of Fig. 6 to be compatible with reduction of glucagon secretion by K(ATP) closure in the physiological range of low glucose.

If α-cells are able to oscillate due to intrinsic mechanisms, glucagon secretion would still be static when uncoupled from paracrine interactions (Fig. 9B). Since α cells are not coupled by gap-junctions like β cells, some other mechanism must exist to synchronize glucagon secretion in order for islets to produce pulses of secretion. We have shown that paracrine effects are sufficient to synchronize glucagon oscillations (Fig. 9D).

Anti-phase oscillations have been seen *in vitro* in high glucose levels (20 mM) (35–38) and *in vivo* (57–59). However the purpose of these asynchronous oscillations is unclear. Perhaps having these oscillations helps keep glucose levels in the appropriate range. It is well known that pulsatile insulin secretion helps the liver function more efficiently. More information is needed about the benefit of pulsatile glucagon secretion. See (60) for a recent review of the literature on this question.

In addition to possibly inadequate coupling (as in Figs. 5, 8, 9), another barrier to pulsatile glucagon secretion is heterogeneity of α-cells. Whereas δ-cells are also presumably heterogeneous, this is likely of less consequence as their secretion depends monotonically on K(ATP) conductance; α-cells in contrast have a non-monotonic dose response curve (Fig. 2B), which allows the direction, as well as the magnitude, of the glucose dependence to vary. Indeed, the results in Figs. 6, 7 depend on the α-cells having the same K(ATP) conductance or at least being tightly clustered in the same region.

Two recent studies have shown, however, that whereas in some α cells cytosolic Ca^{2+} decreased with glucose, the majority increased Ca^{2+} (61, 62). We propose that insulin and/or somatostatin could help suppress α cells that inappropriately secrete at high glucose. However, a full exploration of heterogeneity requires a model with hundreds of α-cells to generate distributions of parameters and outcomes. This is more readily done with a simplified model. Results with such a model (Watts and Sherman, manuscript in preparation) provide additional insight into the potent effects of paracrine factors. For example, in our

previous model (14), the J-shaped secretion dose-response curve observed experimentally (63–65) was obtained by combining the effects of SOC and K(ATP). The simplified model indicates that paracrine effects can offer an alternative explanation for this.

Author Contributions

MW preformed research and wrote paper, OK preformed research, JH preformed research, and AS designed research and wrote paper

Acknowledgments

This work was supported by the Intramural Research Program of the National Institutes of Health (NIDDK).

Table 1: Parameters for the β-cell

$g_{K(Ca),b}$	=	280 pS	$n_{Ca,b}$	=	590
$k_{4,b}$	=	150	$v_{m,b}$	=	-6 mV
$s_{m,b}$	=	10	$g_{Ca,b}$	=	7 pS
$g_{K,b}$	=	1800 pS	τ_n	=	5 ms
$k_{PMCA,b}$	=	0.2 ms^{-1}	$J_{GK,b}$	=	0.4 μM ms^{-1}
B	=	1 ms^{-1}			

Appendix

The β-α-δ (BAD) model combines the dual oscillator model (DOM) for β-cells, our recent α-cell model, a new model for δ-cells, and the interactions between them. Since a complete mathematical description of the DOM and α-cell model has been published previously, only the key elements of the model will be described here. The equations for the interactions between the cells can be found in the main text and the parameters can be found in Table 3.

β-cell Model

The DOM consists of three interacting compartments: Electrical/Calcium, Glycolytic, and Mitochondrial and accounts for the three main oscillatory behaviors of islets: fast electrical bursting, slow glycolytic bursting, and compound bursting. The electrical/calcium component contains the membrane potential (V_b), the Hodgkin-Huxley gating variable for the voltage dependent K^+ channels (n), cytosolic calcium (c_b), Ca^{2+} within a microdomain of L-type Ca^{2+} channels ($c_{mdL,b}$) and Ca^{2+} stored internally in the endoplasmic reticulum (ER) (c_{ER}). The equation for the plasma membrane potential is

$$\frac{dV_b}{dt} = -(I_{K,b} + I_{KCa,b} + I_{K(ATP,b)} + I_{Ca,b} + I_{GIRK,b})/C_{m,b} \tag{13}$$

and the calcium equations for the cell are

$$c_b = f_c(J_R, b + f_{V,b}B(c_{md,b} - c_b) - k_{PMCA,b}(c_b - c_{bas}) + J_{ER,b} + \delta J_m) \tag{14}$$

$$c_{md,b} = f_{md}J_{L,b} - B(c_{md,b} - c_b) \tag{15}$$

where $J_{L,b}$ and $J_{R,b}$ are molar Ca^{2+} influx through open L- and R-type Ca^{2+} channels, f_c and f_{md} are the fraction of free Ca^{2+} in the cytosol and microdomain, B is the transport rate constant of Ca^{2+} between the cytosol and the microdomain, and $J_{ER,b}$ and J_m are Ca^{2+} flux out of the ER and mitochondria.

After entering the cell, glucose is metabolized in glycolysis. It is phosphorylated to glucose-6-phosphate (G6P) by glucokinase (GK), isomerized to fructose-6-phosphate (F6P), then phosphorylated a second time to fructose-1,6-bisphosphate (FBP) by phosphofructokinase-1 (PFK-1), the key enzyme that controls glycolytic oscillations. F6P is assumed to be in equilibrium with G6P; therefore, the equations for the glycolytic component are

$$\begin{aligned} \frac{dG6P}{dt} &= \kappa(J_{GK} - J_{PFK}) \\ \frac{dFBP}{dt} &= \kappa(J_{PFK} - \frac{1}{2}J_{GPDH}). \end{aligned} \tag{16}$$

where J_{PFK} and J_{GPDH} are the PFK and GPDH reaction rates and J_{GK} is the glucokinase rate, which is treated as a parameter of the model

The final component describes the reactions in the mitochondria, which metabolizes the carbons from glucose and produces most of the ATP in the cell. The mitochondrial component has four variables: mitochondrial NADH concentration ($NADH_m$), mitochondrial ADP concentration (ADP_m), mitochondrial calcium concentration (c_m), and the inner membrane potential (ψ_m). We use the rate of glyceraldehyde 3-phosphate dehydrogenase (GPDH), which is in equilibrium with FBP, as the input into the mitochondria. That rate satisfies

$$J_{GPDH} = k_{GPDH}\sqrt{FBP(1\mu M)}. \tag{17}$$

We added a kinetic model for granule exocytosis to the DOM in order to model insulin secretion from the

β-cell. The kinetic model was taken from Chen et al. (17). The exocytosis cascade describes the interaction between the insulin containing granules and the plasma membrane inside the β-cell and is divided into seven steps. It is assumed that a granule has to dock to the membrane from a reserve pool, be primed, and move to the microdomain of an L-type Ca^{2+} channel before it can bind with Ca^{2+} and fuse with the cell membrane. The number of granules in pool *i* is given by the following equations:

$$\begin{aligned}
N_{1,b} &= -[3k_{1,b}c_{mod} + r_{-1,b}]N_{1,b} + k_{-1,b}N_{2,b} + r_{1,b}N_{5,b} \\
N_{2,b} &= 3k_{1,b}c_{mod}N_{1,b} - [2k_{1,b}c_{mod} + k_{-1,b}]N_{2,b} + 2k_{-1,b}N_{3,b} \\
N_{3,b} &= 2k_{1,b}c_{mod}N_{2,b} - [k_{1,b}c_{mod} + 2k_{-1,b}]N_{3,b} + 3k_{-1,b}N_{4,b} \\
N_{4,b} &= k_{1,b}c_{mod}N_{3,b} - [3k_{-1,b} + u_{1,b}]N_{4,b} \\
N_{5,b} &= r_{-1,b}N_{1,b} - [r_{1,b} + r_{-2,b}]N_{5,b} + r_{2,b}N_{6,b} \\
N_{6,b} &= r_{3,b} + r_{-2,b}N_{5,b} - [r_{-3,b} + r_{2,b}]N_{6,b} \\
N_{F,b} &= u_{1,b}N_{4,b} - u_{2,b}N_{F,b} \\
N_{R,b} &= u_{2,b}N_{F,b} - u_{3,b}N_{R,b}
\end{aligned} \tag{18}$$

States 1-6 contain vesicles in the docked and primed states, state F is the number of granules in the fused state, and state R is the number of granules ready to be released. The resupply rate (r_{3b}) is assumed to be modulated through an amplifying signal generated from glucose metabolism or other cellular reactions. Here the amplifying signal comes from the mitochondrial compartment. Specifically, the variable J_O which is the oxygen consumption at the final stage of the electron transport chain, during which NADH is converted to NAD^+. We use this variable because mitochondrial metabolism has been shown to be important for amplification of insulin secretion (66). The equation for the resupply rate is:

$$r_{3,b} = 0.032 + 14J_O^2\, r_3^0\, \frac{c_b}{c_b + K_p}. \tag{19}$$

In order to add exocytosis to the DOM, microdomain calcium was modified by the following equation:

$$c_{mod} = \frac{0.06935 + 32c_{md}^4}{c_{md}^4 + 81}. \tag{20}$$

This function scales the Ca^{2+} in the microdomain to be more in-line with the microdomain Ca^{2+} concentrations used in (17). The rate of insulin secretion J_{IS} is given by the following equation:

$$J_{IS} = 0.0016 u_{3,b} N_R. \tag{21}$$

Parameters which have been changed from (15–17) can be found in Table 1.

α-cell Model

Unlike the β-cell model, the α-cell model (14) currently contains only one compartment: the electrical/calcium. There are 15 variables: the membrane potential (V_a), the Hodgkin-Huxley gating variables for the voltage-dependent Ca^{2+} and K^+ channels, cytosolic Ca^{2+} (c_a), Ca^{2+} within the microdomain of N-type Ca^{2+} channels ($c_{mdN,a}$), and Ca^{2+} stored in the ER ($c_{ER,a}$). The equation for the plasma membrane potential (V_a) is

$$\frac{dV_a}{dt} = -(I_{K,a} + I_{Ka,a} + I_{K(ATP,a)} + I_{CaL,a} + I_{CaN,a} + I_{CaT,a} + I_{Na,a} + I_{L,a} + I_{SOC,a} + I_{GIRK,a})/C_{m,a}. \tag{22}$$

and the calcium equations for the cell are

$$\begin{aligned} c_a &= f_c(J_{T,a} + J_{L,a} + f_{V,a}B(c_{mdN,a} - c_a) - k_{PMCA,a}c_a + J_{ER,a}) \\ c_{mdN,a} &= f_{md,a}J_{N,a} - f_{md,a}B(c_{mdN,a} - c_a) \\ c_{er,a} &= -f_{er}(V_{cyt}/V_{er})[p_l(c_{er,a} - c_a) - k_{SERCA}c_a] \end{aligned} \tag{23}$$

where $J_{T,a}$, $J_{L,a}$, and $J_{N,a}$ are molar Ca^{2+} influx through open T-, L-, and N-type Ca^{2+} channels.

The kinetic model for granule exocytosis was added to the α-cell model as a replacement for the glucagon secretion equations. This change was necessary to model somatostatin's effect on exocytosis. The equations are the same as the β-cell equations (see Eq. 18 above) with the exception that we do not include a mitochondrial compartment and assume that the resupply rate ($r_{3,a}$) depends only on calcium:

$$r_{3,a} = 0.05 r_{3,a}^{0} \frac{c_a}{c_a + K_p}. \tag{24}$$

The rate of glucagon secretion is:

$$J_{GS} = 0.0000988 u_{3,a} N_{R,a}. \tag{25}$$

In order to test the effects of heterogeneity on glucagon oscillations (Figs. 7 & 8) we added the glycolytic compartment from (15) to the α-cell model. Along with the equations for G6P and FBP (Eqns. 4 & 5), the following equation for ADP was added:

$$\frac{dADP_a}{dt} = (ATP_a - ADP_a \exp[\gamma(1 - c_a/0.45)])/\tau_a \tag{26}$$

where γ is given by the following equation:

$$\gamma = \frac{8 J_{GPDH}}{k_\gamma + J_{GPDH}} \tag{27}$$

ADP is affected by cytosolic Ca^{2+} and glycolysis. The Ca^{2+} effect is through the factor $(1 - c_a/0.45)$, while input from glycolysis is incorporated through γ.

Table 2: Parameters for the δ-cell

$g_{Na,d}$	=	5 nS	$g_{CaN,d}$	=	0.7 nS
$g_{KA,d}$	=	0.5 nS	$g_{K.d}$	=	7.5 nS
$v_{CaN,d}$	=	-15 mV	k_{PQ}	=	40
N_{PQ}	=	0.1	$f_{Vl,d}$	=	0.00340
$f_{Vpq,d}$	=	0.00226			

δ-cell Model

The δ-cell model was modified from the α-cell model in (14), and contains 13 variables because there are no T-type Ca^{2+} channels. The equation for the plasma membrane potential (V_d) is

$$\frac{dV_d}{dt} = -(I_{K,d} + I_{Ka,d} + I_{K(ATP,d)} + I_{CaL,d} + I_{CaN,d} + I_{Na,d} + I_{L,d} + I_{GABA,d})/C_{m,d} \tag{28}$$

and the calcium equations for the cell are

$$\begin{aligned} c_d &= f_c(f_{Vl,d}B(c_{mdL,d} - c_d) + f_{Vpq,d}B(c_{mdPQ,d} - c_d) - k_{PMCA,d}c_d + J_{ER,d}) \\ c_{mdPQ,d} &= f_{md,d}J_{PQ,d} - f_{md,d}B(c_{mdPQ,d} - c_d) \\ c_{mdL,d} &= f_{md,d}J_{L,d} - f_{md,d}B(c_{mdL,d} - c_d) \\ c_{er,d} &= -f_{er}(V_{cyt}/V_{er})[p_l(c_{er,d} - c_d) - k_{SERCA,d}c_d] \end{aligned} \tag{29}$$

We modeled somatostatin secretion as depending on Ca^{2+} in the microdomains surrounding P/Q type Ca^{2+} channels since these channels have been linked to somatostatin secretion (67). The rate of secretion is expressed as

$$J_{SS} = N_{PQ}\, m_{CaPQ}\, h_{CaPQ} \left(\frac{C_{mdPQ}}{k_{PQ} + C_{mdPQ}}\right)^4, \tag{30}$$

following the formulation in Pedersen and Sherman (68). For Fig. 4, we assume that somatostatin secretion responds to glucose via a K(ATP)-independent amplifying factor. In this case, the secretion equation

Table 3: Parameters for Paracrine Interactions

f_b	=	2000	f_a	=	150
f_d	=	0.003	$\bar{g}_{GABA}$	=	0.1 nS
v_{GABA}	=	0 mV	$\bar{g}_{GIRK,a}$	=	0.025 nS
$\bar{g}_{GIRK,b}$	=	10 pS	V_{GIRK}	=	-80 mV
r_a	=	5 s^{-1}	r_b	=	0.002 s^{-1}

becomes

$$J_{SS} = Amp\, N_{PQ}\, m_{CaPQ}\, h_{CaPQ} \left(\frac{C_{mdPQ}}{k_{PQ} + C_{mdPQ}} \right)^4, \tag{31}$$

where Amp = 1 in 1 G and 2 in 7 G.

Table 2 lists the parameter values which differ from the α-cell model.

References

[1] Gromada, J., I. Franklin, and C. B. Wollheim, 2007. α-cells of the endocrine pancreas: 35 years of research but the enigma remains. Endocr Rev 28:84–116.

[2] MacDonald, P. E., Y. Z. D. Marinis, R. Ramracheya, A. Salehi, X. Ma, P. R. Johnson, R. Cox, L. Eliasson, and P. Rorsman, 2007. A K_{ATP} channel-dependent pathway within α-cells regulates glucagon release from both rodent and human islets of langerhans. PLoS Biol. 5:1236–1247.

[3] Liu, Y. J., E. Vieira, and E. Gylfe, 2004. A store-operated mechanism determines the activity of the electrically excitable glucagon-secreting pancreatic α-cell. Cell Calcium 35:357–65.

[4] Maruyama, H., A. Hisatomi, L. Orci, G. M. Grodsky, and R. H. Unger, 1984. Insulin within islets is a physiologic glucagon release inhibitor. J. Clin. Invest. 74:2296–2299.

[5] Samols, E., and J. I. Stagner, 1988. Intra-islet regulation. Am. J. Med. 85:31–35.

[6] Ishihara, H., P. Maechler, A. Gjinovci, P. L. Herrera, and C. B. Wollheim, 2003. Islet β-cell secretion determines glucagon release from neighbouring α-cells. Nat Cell Biol 5:330–5.

[7] Franklin, I., J. Gromada, A. Gjinovci, S. Theander, and C. B. Wollheim, 2005. β-cell secretory products activate α-cell ATP-dependent potassium channels to inhibit glucagon release. Diabetes 54:1808–15.

[8] Franklin, I. K., and C. B. Wollheim, 2004. GABA in the endocrine pancreas: its putative role as an islet cell paracrine-signalling molecule. J Gen Physiol 123:185–90.

[9] Wendt, A., B. Birnir, K. Buschard, J. Gromada, A. Salehi, S. Sewing, P. Rorsman, and M. Braun, 2004. Glucose inhibition of glucagon secretion from rat α-cells is mediated by [GABA] released from neighboring β-cells. Diabetes 53:1038–45.

[10] Rorsman, P., P. O. Berggren, K. Bokvist, H. Ericson, H. Mohler, C. G. Ostenson, and P. A. Smith, 1989. Glucose-inhibition of glucagon secretion involves activation of [GABAA]-receptor chloride channels. Nature 341:233–6.

[11] Gerich, J. E., R. Lovinger, and G. M. Grodsky, 1975. Inhibition by somatostatin of glucagon and insulin release from the perfused rat pancreas in reponse to arginine, isoproterenol and theophylline: evidence for a preferential effect on glucagon secretion. Endocrinology 96:749–754.

[12] Strowski, M. Z., R. M. Parmar, A. D. Blake, and J. M. Schaeffer, 2000. Somatostatin inhibits insulin and glucagon secretion via two receptors subtypes: an in vitro study of pancreatic islets from somatostatin receptor 2 knockout mice. Endocrinology 141:111–117.

[13] Hauge-Evans, A. C., A. J. King, D. Carmignac, C. C. Richardson, I. C. Robinson, M. J. Low, M. R. Christie, S. J. Persaud, and P. M. Jones, 2009. Somatostatin secreted by islet δ-cells fulfills multiple roles as a paracrine regulator of islet function. Diabetes 58:403–11.

[14] Watts, M., and A. Sherman, 2014. Modeling the pancreatic α-cell: dual mechanisms of glucose suppression of glucagon secretion. Biophys J 106:741–51.

[15] Bertram, R., L. Satin, M. Zhang, P. Smolen, and A. Sherman, 2004. Calcium and glycolysis mediate multiple bursting models in pancreatic islets. Biophys. J. 87:3074–3087.

[16] Bertram, R., A. Sherman, and L. S. Satin, 2007. Metabolic and electrical oscillations: partners in controlling pulsatile insulin secretion. Am J Physiol Endocrinol Metab 293:E890–900.

[17] Chen, Y. D., S. Wang, and A. Sherman, 2008. Identifying the targets of the amplifying pathway for insulin secretion in pancreatic beta-cells by kinetic modeling of granule exocytosis. Biophys J 95:2226–41.

[18] Göpel, S. O., T. Kanno, S. Barg, and P. Rorsman, 2000. Patch-clamp characterisation of somatostatin-secreting δ-cells in intact mouse pancreatic islets. J. Pysiol. 528:497–507.

[19] Leung, Y. M., I. Ahmed, L. Sheu, X. Gao, M. Hara, R. G. Tsushima, N. E. Diamant, and H. Y. Gaisano, 2006. Insulin regulates islet α-cell function by reducing KATP channel sensitivity to adenosine 5'-triphosphate inhibition. Endocrinology 147:2155–62.

[20] Elliott, A. D., A. Ustione, and D. W. Piston, 2014. Somatostatin and Insulin Mediate Glucose-Inhibited Glucagon Secretion in the Pancreatic -Cell by Lowering cAMP. Am. J. Physiol. Endocrinol. Metab. ajpendo.00344.2014.

[21] Brunicardi, F. C., R. Kleinman, S. Moldovan, T. H. Nguyen, P. C. Watt, J. Walsh, and R. Gingerich, 2001. Immunoneutralization of somatostatin, insulin, and glucagon causes alterations in islet cell secretion in the isolated perfused human pancreas. Pancreas 23:302–8.

[22] Braun, M., A. Wendt, J. Karanauskaite, J. Galvanovskis, A. Clark, P. E. MacDonald, and P. Rorsman, 2007. Corelease and differential exit via the fusion pore of GABA, serotonin, and ATP from LDCV in rat pancreatic beta cells. J Gen Physiol 129:221–31.

[23] Braun, M., R. Ramracheya, M. Bengtsson, A. Clark, J. N. Walker, P. R. Johnson, and P. Rorsman, 2010. Gamma-aminobutyric acid (GABA) is an autocrine excitatory transmitter in human pancreatic β-cells. Diabetes 59:1694–701.

[24] Yoshimoto, Y., Y. Fukuyama, Y. Horio, A. Inanobe, M. Gotoh, and Y. Kurachi, 1999. Somatostatin induces hyperpolarization in pancreatic islet a cells by activating a G protein-gated K+ channel. Febs Letters 444:265–269.

[25] Gromada, J., M. Hoy, K. Buschard, A. Salehi, and P. Rorsman, 2001. Somatostatin inhibits exocytosis in rat pancreatic α-cells by G(i2)-dependent activation of calcineurin and depriming of secretory granules. J Physiol 535:519–32.

[26] Gromada, J., M. Hoy, H. L. Olsen, C. F. Gotfredsen, K. Buschard, P. Rorsman, and K. Bokvist, 2001. Gi2 proteins couple somatostatin receptors to low-conductance $[K]^+$ channels in rat pancreatic α-cells. Pflugers Arch 442:19–26.

[27] Kailey, B., M. van de Bunt, S. Cheley, P. R. Johnson, P. E. MacDonald, A. L. Gloyn, P. Rorsman, and M. Braun, 2012. SSTR2 is the functionally dominant somatostatin receptor in human pancreatic β- and α-cells. Am J Physiol Endocrinol Metab 303:E1107–16.

[28] Claro, A., V. Grill, S. Efendic, and R. Luft, 1977. Studies on the mechanisms of somatostatin action on insulin release. IV. effect of somatostatin on cyclic AMP levels and phosphodiesterase activity in isolated rat pancreatic islets. Acta Endocrinol (Copenh) 85:379–88.

[29] Schuit, F. C., and D. G. Pipeleers, 1985. Regulation of adenosine 3',5'-monophosphate levels in the pancreatic B cell. Endocrinology 117:834–40.

[30] Ikeuchi, M., and D. L. Cook, 1984. Glucagon and forskolin have dual effects upon islet cell electrical activity. Life Sci 35:685–91.

[31] Samols, E., G. Marri, and V. Marks, 1965. Promotion of Insulin Secretion by Glucagon. Lancet 2:415–6.

[32] Ermentrout, B., 2002. Simulating, analyzing, and animating dynamical systems: A guide to XPPAUT for researchers and students. SIAM, Philadelphia.

[33] Cheng-Xue, R., A. Gomez-Ruiz, N. Antoine, L. A. Noel, H. Y. Chae, M. A. Ravier, F. Chimienti, F. C. Schuit, and P. Gilon, 2013. Tolbutamide Controls Glucagon Release From Mouse Islets Differently Than Glucose: Involvement of KATP Channels From Both α-Cells and δ-Cells. Diabetes 62:1612–22.

[34] Zhang, Q., M. Bengtsson, C. Partridge, A. Salehi, M. Braun, R. Cox, L. Eliasson, P. R. V. Johnson, E. Renstrm, T. Schneider, P.-O. Berggren, S. Gpel, F. M. Ashcroft, and P. Rorsman, 2007. R-type Ca^{2+}-channel-evoked CICR regulates glucose-induced somatostatin secretion. Nat. Cell Biol. 9:453–460.

[35] Hellman, B., A. Salehi, E. Gylfe, H. Dansk, and E. Grapengiesser, 2009. Glucose generate coincident insulin and somatostatin pulses and antisynchronous glucagon pulses from human pancreatic islets. Endocrinology 150:5334–5340.

[36] Hellman, B., A. Salehi, E. Grapengiesser, and E. Gylfe, 2012. Isolated mouse islets respond to glucose with an initial peak of glucagon release followed by pulses of insulin and somatostatin in antisynchrony with glucagon. Biochem. Biophys. Res. Commun. 417:1219–1223.

[37] Salehi, A., S. S. Qader, E. Grapengiesser, and B. Hellman, 2007. Pulses of somatostatin release are slightly delayed compared with insulin and antisynchronous to glucagon. Regulatory Peptides 144:43–49.

[38] Grapengiesser, E., A. Salehi, S. S. Qader, and B. Hellman, 2006. Glucose induces glucagon release pulses antisynchronous with insulin and sensitive to purinoceptor inhibition. Endocrinology 147:3472–7.

[39] Bertram, R., L. Satin, M. G. Pedersen, D. Luciani, and A. Sherman, 2007. Interaction of glycolysis and mitochondrial respiration in metabolic oscillations of pancreatic islets. Biophys. J. 92:1544–1555.

[40] Tornheim, K., 1997. Are metabolic oscillations responsible for normal oscillatory insulin secretion? Diabetes 46:1375–80.

[41] Benninger, R. K., M. Zhang, W. S. Head, L. S. Satin, and D. W. Piston, 2008. Gap junction coupling and calcium waves in the pancreatic islet. Biophys J 95:5048–61.

[42] Benninger, R. K., W. S. Head, M. Zhang, L. S. Satin, and D. W. Piston, 2011. Gap junctions and other mechanisms of cell-cell communication regulate basal insulin secretion in the pancreatic islet. J Physiol 589:5453–66.

[43] Head, W. S., M. L. Orseth, C. S. Nunemaker, L. S. Satin, D. W. Piston, and R. K. Benninger, 2012. Connexin-36 gap junctions regulate in vivo first- and second-phase insulin secretion dynamics and glucose tolerance in the conscious mouse. Diabetes 61:1700–7.

[44] Berts, A., E. Gylfe, and B. Hellman, 1995. $[Ca]^{2+}$ oscillations in pancreatic islet cells secreting glucagon and somatostatin. Biochem Biophys Res Commun 208:644–9.

[45] Berts, A., A. Ball, E. Gylfe, and B. Hellman, 1996. Suppression of $[Ca]^{2+}$ oscillations in glucagon-producing α 2-cells by insulin/glucose and amino acids. Biochim Biophys Acta 1310:212–6.

[46] Quesada, I., M. G. Todorova, P. Alonso-Magdalena, M. Beltra, E. M. Carneiro, F. Martin, A. Nadal, and B. Soria, 2006. Glucose induces opposite intracellular $[Ca]^{2+}$ concentration oscillatory patterns in identified α- and β-cells within intact human islets of Langerhans. Diabetes 55:2463–9.

[47] Nadal, A., I. Quesada, and B. Soria, 1999. Homologous and heterologous asynchronicity between identified α-, β- and δ-cells within intact islets of Langerhans in the mouse. J Physiol 517 (Pt 1):85–93.

[48] Zhang, Q., R. Ramracheya, C. Lahmann, A. Tarasov, M. Bengtsson, O. Braha, M. Braun, M. Brereton, S. Collins, J. Galvanovskis, A. Gonzalez, L. N. Groschner, N. J. Rorsman, A. Salehi, M. E. Travers, J. N. Walker, A. L. Gloyn, F. Gribble, P. R. Johnson, F. Reimann, F. M. Ashcroft, and P. Rorsman, 2013. Role of [KATP] channels in glucose-regulated glucagon secretion and impaired counterregulation in type 2 diabetes. Cell Metab 18:871–82.

[49] Li, J., Q. Yu, P. Ahooghalandari, F. M. Gribble, F. Reimann, A. Tengholm, and E. Gylfe, 2015. Submembrane ATP and Ca2+ kinetics in α-cells: unexpected signaling for glucagon secretion. FASEB J. .

[50] Nadal, A., I. Quesada, and B. Soria, 1999. Homologous and heterologous asynchronicity between identified alpha-, beta- and delta-cells within intact islets of Langerhans in the mouse. J. Physiol. (Lond.) 517 (Pt 1):85–93.

[51] Quoix, N., R. Cheng-Xue, L. Mattart, Z. Zeinoun, Y. Guiot, M. C. Beauvois, J. C. Henquin, and P. Gilon, 2009. Glucose and pharmacological modulators of ATP-sensitive K+ channels control [Ca2+]c by different mechanisms in isolated mouse alpha-cells. Diabetes 58:412–21.

[52] Huang, Y. C., M. Rupnik, and H. Y. Gaisano, 2011. Unperturbed islet alpha-cell function examined in mouse pancreas tissue slices. J Physiol 589:395–408.

[53] Dadi, P. K., B. Luo, N. C. Vierra, and D. A. Jacobson, 2015. TASK-1 Potassium Channels Limit Pancreatic -Cell Calcium Influx and Glucagon Secretion. Mol. Endocrinol. 29:777–787.

[54] Kailey, B., M. van de Bunt, S. Cheley, P. R. Johnson, P. E. MacDonald, A. L. Gloyn, P. Rorsman, and M. Braun, 2012. SSTR2 is the functionally dominant somatostatin receptor in human pancreatic - and -cells. Am. J. Physiol. Endocrinol. Metab. 303:E1107–1116.

[55] Gylfe, E., and A. Tengholm, 2014. Neurotransmitter control of islet hormone pulsatility. Diabetes Obes Metab 16 Suppl 1:102–10.

[56] van der Meulen, T., C. J. Donaldson, E. Cceres, A. E. Hunter, C. Cowing-Zitron, L. D. Pound, M. W. Adams, A. Zembrzycki, K. L. Grove, and M. O. Huising, 2015. Urocortin3 mediates somatostatin-dependent negative feedback control of insulin secretion. Nat. Med. 21:769–776.

[57] Menge, B. A., L. Gruber, S. M. Jorgensen, C. F. Deacon, W. E. Schmidt, J. D. Veldhuis, J. J. Holst, and J. J. Meier, 2011. Loss of inverse relationship between pulsatile insulin and glucagon secretion in patients with type 2 diabetes. Diabetes 60:2160–8.

[58] Lang, D. A., D. R. Matthews, M. Burnett, G. M. Ward, and R. C. Turner, 1982. Pulsatile, synchronous basal insulin and glucagon secretion in man. Diabetes 31:22–6.

[59] Goodner, C. J., B. C. Walike, D. J. Koerker, J. W. Ensinck, A. C. Brown, E. W. Chideckel, J. Palmer, and L. Kalnasy, 1977. Insulin, glucagon, and glucose exhibit synchronous, sustained oscillations in fasting monkeys. Science 195:177–9.

[60] Satin, L. S., P. C. Butler, J. Ha, and A. S. Sherman, 2015. Pulsatile insulin secretion, impaired glucose tolerance and type 2 diabetes. Mol. Aspects Med. .

[61] Le Marchand, S. J., and D. W. Piston, 2010. Glucose suppression of glucagon secretion: metabolic and calcium responses from α-cells in intact mouse pancreatic islets. J Biol Chem 285:14389–98.

[62] Le Marchand, S. J., and D. W. Piston, 2012. Glucose decouples intracellular $[Ca]^{2+}$ activity from glucagon secretion in mouse pancreatic islet α-cells. PLoS One 7:e47084.

[63] Walker, J. N., R. Ramracheya, Q. Zhang, P. R. Johnson, M. Braun, and P. Rorsman, 2011. Regulation of glucagon secretion by glucose: paracrine, intrinsic or both? Diabetes Obes Metab 13 Suppl 1:95–105.

[64] Salehi, A., E. Vieira, and E. Gylfe, 2006. Paradoxical stimulation of glucagon secretion by high glucose concentrations. Diabetes 55:2318–23.

[65] Vieira, E., A. Salehi, and E. Gylfe, 2007. Glucose inhibits glucagon secretion by a direct effect on mouse pancreatic α cells. Diabetologia 50:370–9.

[66] MacDonald, M. J., L. A. Fahien, L. J. Brown, N. M. Hasan, J. D. Buss, and M. A. Kendrick, 2005. Perspective: emerging evidence for signaling roles of mitochondrial anaplerotic products in insulin secretion. Am J Physiol Endocrinol Metab 288:E1–15.

[67] Braun, M., R. Ramracheya, S. Amisten, M. Bengtsson, Y. Moritoh, Q. Zhang, P. R. Johnson, and P. Rorsman, 2009. Somatostatin release, electrical activity, membrane currents and exocytosis in human pancreatic delta cells. Diabetologia 52:1566–78.

[68] Pedersen, M. G., and A. Sherman, 2009. Newcomer insulin secretory granules as a highly calcium-sensitive pool. Proc Natl Acad Sci U S A 106:7432–6.